

The hollow spherical nano-TiO₂ particles synthesized from Ti-bearing blast furnace slag and the reaction model analysis

H. H. Yu^{a,b}, W.Z. Zhou^a, X.Li^{a,*}

^a*School of Material Science and Engineering, Shenyang Ligong University, Shenyang 110159, China*

^b*School of Metallurgy, Northeastern University, Shenyang 110004, China*

The hollow spherical nano-TiO₂ was successfully synthesized by carbon spheres as the template and Ti-bearing blast furnace slag as the Ti source. The SEM and TEM results showed that the as-synthesized TiO₂ consist of uniform separated hollow spheres, and the sphere wall was composed of nanoparticles. The XRD result showed that the crystallized phase was rutile. Almost complete extraction of Ti from slag was achieved in NaOH-NaF molten salt. The kinetic analysis indicated that the slag decomposition was applied to control of chemical reaction of the reactionless core-shrinking model, and the apparent activation energy was 39.54 kJ mol⁻¹.

(Received November 26, 2020; Accepted April 30, 2021)

Keywords: Ti-bearing blast furnace slag, Kinetic, TiO₂, Molten salt

1. Introduction

Nano-TiO₂ with hollow structures are believed to be able to provide an increase surface/volume ratio and decrease of the lengths of transport for the transmission of charge and mass, which has a variety of applications in dye-sensitized solar cells, photocatalysis, fuel cells, lithium ion batteries, and supercapacitors [1-4]. Hollow structures TiO₂ can be prepared by using different precursors, for example TiCl₄, TBT, Ti(NO₃)₄ or Ti(SO₄)₂. With the higher cost of precursors, the cost of TiO₂ is higher.

There are amount of V-Ti resources deposited in the southwest of China [5, 6]. At present, approximately 53 percent of the Ti is separated from blast furnaces ironmaking process and enters the blast furnaces slag, in which the content of TiO₂ contains 19.0 – 23.0 %. This slag is called Ti-bearing blast furnace slag (TFS). TFS as solid waste is piled up, that is an obvious waste of Ti resource in past. Now, it is the direct source for Ti extraction.

In the past, many methods such as sulfuric acid process and hydrochloric acid process had been applied to treating TFS [7-12]. Due to difficulty for breaking the strong Ti-O bond in perovskite phases, these methods were proved to low Ti extraction rate. So, the method of separating Ti by enriching Ti components into specific crystal phases is proposed. Sui et al. [13-16] carried out a large of studies on the transfer of components of Ti into perovskite phase. By the flotation method, the phase can be separated from TFS and the TiO₂ content can be enhancement to 35.0 – 45.0 wt.%. Zhang [17, 18] et al obtained rutile crystal TiO₂ by high-temperature modification and the content of Ti in rutile phase was about 65.0 wt.%. In addition to the high operating temperature, the leaching rate is only about 60 wt% by crystallographic enrichment. It is still necessary to find a treatment method with mild conditions and high leaching rate.

In this study, a novel method to extract Ti from TFS using NaOH-NaF molten salt was proposed and the kinetic process of the molten salt reaction process is analyzed in detail. The hollow spherical TiO₂ materials using TFS as Ti precursors was green synthesized.

* Corresponding author: lx80ws@126.com

2. Experimental

The chemical reagents used in the experiment were of analytical grade. TFS was used by Pangang Group Co., Ltd. and mainly containing TiO₂ 19.23%, CaO 24.92%, Al₂O₃ 13.64%, MgO 8.04% and SiO₂ 27.74%. In the typical experiments procedure, the 10.0 g of TFS was mixed with the NaOH and NaF. The mixtures was sintered at the temperature range of 425-500°C for time range of 0.5-5 h. To determine TiO₂ extraction efficiency, the roasted sample was dissolved by 5 wt. % HCl. After the complete dissolution of the sample, unreacted residues were separated from the solution by filtration because it could not be dissolved in the diluted HCl solution. The titanium extraction was calculated by the following formula:

$$X \% = V \times \frac{T_{Ti}}{m_p} \times \frac{M_i}{M_t} \times C_{Ti} \times 100 \quad (1)$$

where $X\%$ is the titanium fractional conversion, T_{Ti} is the titanium concentration in HCl solution measured by ICP-OES after the dissolution of the product (g L^{-1}), M_t and M_i are the total mass of the reaction product and titanium slag respectively (g), m_p is the mass of the product sample dissolved in HCl solution (g), $C_{Ti}\%$ is the titanium mass fraction in the slag, V is the volume of HCl solution used to dissolve the product sample (L).

Synthesis of hollow spherical nano-TiO₂. Carbon spheres were prepared by the method of reference [16]. A mixture of carbon spheres, deionized water and Ti extraction solution were hydrothermally reacted at 180 °C for 10 h. The reaction product was separated at 5000 rpm by centrifugation. The separated samples was dried at 85 °C for 3 h. And then, the precursor was heated at 700 °C for 3 hours to obtain the TiO₂ product.

In all the experiments, the content of Ti was detected by ICP-OES (Perkin-Elmer, USA). By using XRD (Rigaku D/max- RB) with Cu K-radiation, the crystalline structure of the sample was determined. SEM images of samples were carried out at Hitachi S-3400N. TEM images of the samples were observed on a FEI-F20.

3. Results and discussion

3.1. The conditions analysis on the Ti extraction process

The crucial conditions of roasting process is to control Na₂TiO₃ phase extent, that means to optimize reaction conditions including temperature, particle size and liquid-to-solid ratio (R: the ratio of total mass of sodium hydroxide and sodium fluoride and the total mass of TFS according to the liquid phase formation zone in the phase diagram). The reaction temperature of molten roasting process is crucial parameter, which was carried out from 425 °C to 500 °C (Fig. 1).

In Fig. 1, the extraction of Ti gradually increase with the increasing of reaction temperature and exhibits a similar dependence for each selected temperature. In addition, the viscosity of reaction system is decreased with the increase of reaction temperature, which facilitates the reactants transportation and accelerate the TFS decomposition. The Ti extraction achieves 100.0% when the reaction temperature is 500°C and the reaction time is over 3 h. But, the Ti extraction is only about 92% by dilute sulfuric acid leaching[19].

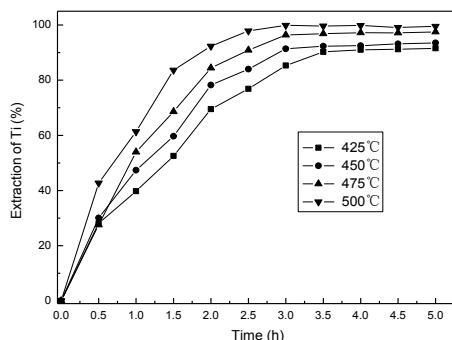


Fig. 1. Effect of temperature on Ti extraction.

Previous studies showed that the silicon-containing phase is a main reason hindering the decomposition of titanium-containing phases[20]. Acidic silica and metal oxides would readily react with NaOH and NaF. The liquid-to-solid ratio (R) is another key parameter for molten roasting, which has been optimized from 1:1 to 3:1 (Fig. 2). The results show that the Ti extractions significantly change with the increase of R, and an increase in conversion is observed. At the reaction temperatures, which are higher than the eutectic temperature of NaF and NaOH, NaOH/NaF and TFS exist as liquid and solid, respectively. It is believed that the higher R decrease the reacting slurry viscosity, and promotes mass transfer of the products and reactants. At the same time, as the R increases, the surface of contact increases between NaOH/NaF and TFS, and reaction is prompted by the increasing of contact surface. Therefore, the Ti extraction efficiency increases significantly with increasing R.

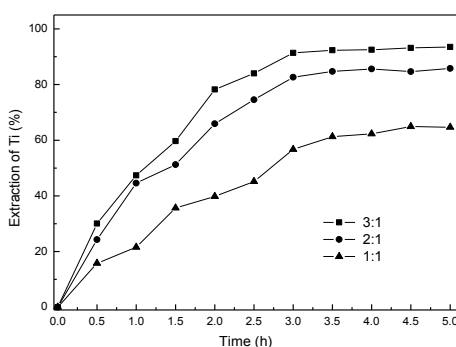


Fig. 2. Effect of The liquid-to-solid ratio (R) on Ti extraction at 425 °C

With the particle size of 100-150 μm , 75-100 μm , 45~75 μm , the effect of particle size on extraction of Ti is investigated and the results are shown in Fig. 3. The extraction of Ti is observed to increase with decreasing particle size, which is attributed to the reason that the specific surface of TFS is increased by the decrease of the particle size. The contact between TFS and liquid is promoted by the increase of solid reactant surface area, which improves the efficiency of reaction. In addition, since the product layer around the smaller particles is thinner, it produce less diffusion resistance and facilitate the transport of the reactants and ultimately increased the reaction rate.

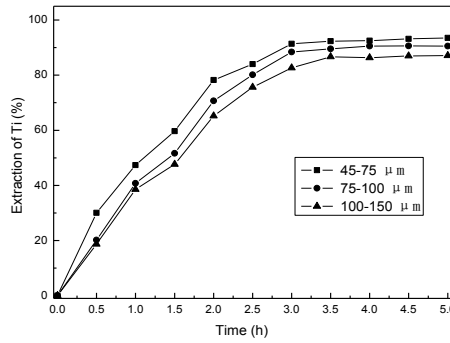


Fig. 3. Effect of particle size on Ti extraction at 425 °C

3.2. The kinetics analysis on the extraction Ti process

The kinetic parameters of Ti extraction from TFS can be obtained by the reactionless core-shrinking model [21]. Under the control of different reaction processes, the dynamic equation can be described as follows:

1. The control of liquid diffusion boundary Layer

$$X = \frac{3MK_M C_A}{\rho r} t = k_1 t \tag{2}$$

2. The control of solid diffusion product Layer

$$1 + 2(1 - X) - 3(1 - X)^{2/3} = \frac{6bMDC_A}{\rho r^2} t = k_2 t \tag{3}$$

3. The control of chemical reaction

$$1 - (1 - X)^{1/3} = \frac{MK_C C_A}{\rho r} t = k_3 t \tag{4}$$

where X is the Ti extraction at time t, M is the molecular weight of TFS, k_M is the mass transfer coefficient of the cluster from reagents in liquid boundary layer, K_C is the first-order rate constant, C_A is the solution concentration, ρ is the density of the particle, r is the initial radius of the particle, D is the diffusion coefficient, b is the stoichiometric coefficient, and k_1, k_2, k_3 are the apparent rate constants.

In order to reveal the control steps of extraction of Ti, as shown in Fig. 4, the extraction X of Ti at 425 °C in Fig. 1 are fitted Equation 2, 3 and 4. The results show that Eq. (4) has a better linear trend in the range of time studied at the selected temperature.

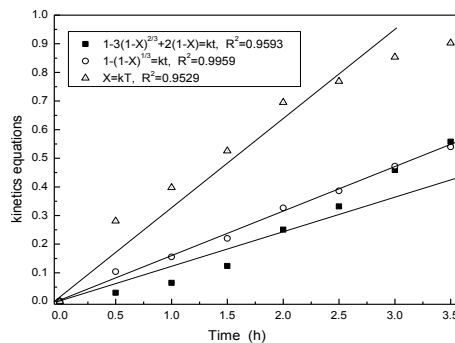


Fig. 4. X, $1 + 2(1 - X) - 3(1 - X)^{2/3}$ and $1 - (1 - X)^{1/3}$ vs. Time.

As shown in Fig. 4, the $1 - (1-X)^{1/3}$ versus time curve show that the Ti extraction at 425-500 °C has a good correlation with the kinetic Eq. (4) for the control of chemical reaction. Therefore, in the NaOH-NaF system, the TFS decomposition is generally controlled by chemical reaction process.

As shown in Fig. 5, the extraction of Ti is fitted according to Eq. (5) at different temperatures and the value of the reaction rate constant k can be obtained from the figure. And then, as shown in Fig. 6, by Arrhenius Eq.(5) the apparent activation energy can be calculated.

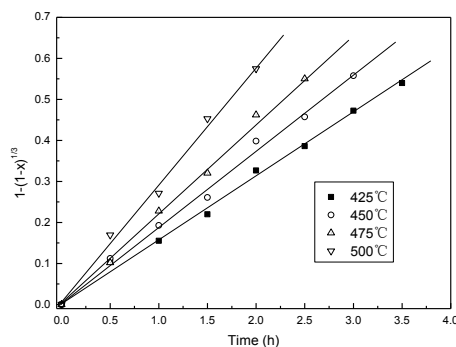


Fig. 5. The fitted plot of $1-(1-X)^{1/3}$ and time.

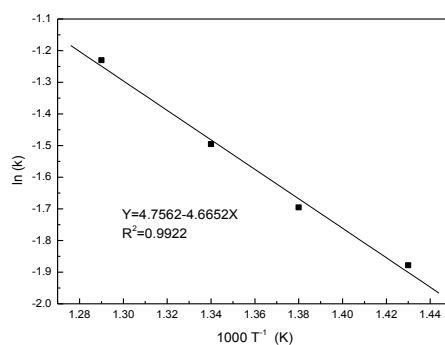


Fig. 6. Activation energy plot of decomposition process.

$$\ln(k) = \ln(A) - \frac{E}{(R \times T)} \quad (5)$$

where k was the reaction rate constant, A was the pre exponential factor, E is the apparent activation energy and R was the gas molar constant. According to the fitting result, E of TFS decomposition reaction is $39.54 \text{ kJ mol}^{-1}$.

3.3. Characterization results of prepared TiO_2 samples

The XRD pattern in Fig. 7 indicates the well crystallized rutile phase is obtained. As shown in Fig. 7, it indicates that the prepared TiO_2 sample has a well-crystallized rutile phase in contrast to the rutile crystal in JCPDF71-167. Fig. 8(a) is the SEM of particles prepared by post annealing at 700 °C for 3 h. It shows that the as-prepared samples also consist of uniform separated hollow spheres with diameter of about ca. 0.9 - 1.2 μm . It shows that the sintered TiO_2 are all hollow structures, and the diameter of the spheres is about 1.0 μm . The TEM image in Fig.8(b) shows that the sample forms a hollow spheres microstructure, and the sphere wall is composed of nanoparticles.

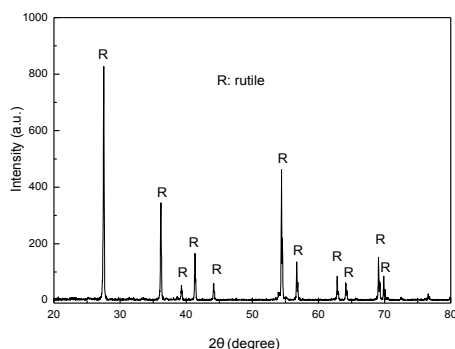


Fig. 7. The XRD pattern of prepared TiO_2 .

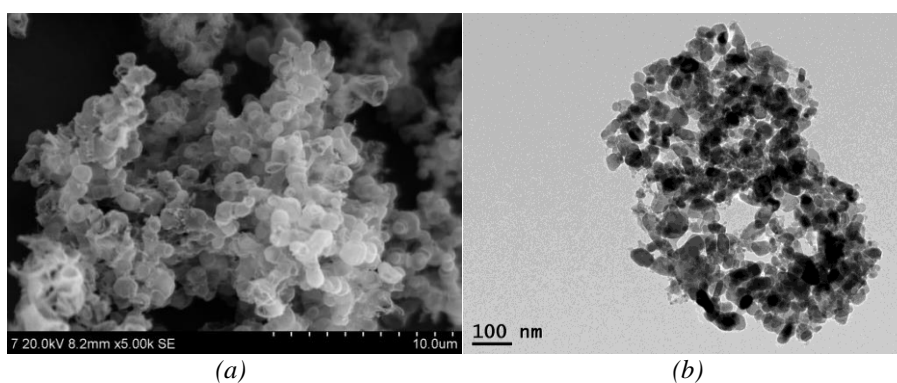


Fig.8. (a) SEM image of TiO_2 (b) TEM image of TiO_2 .

4. Conclusions

In this study, the hollow spherical TiO_2 nanoparticles are synthesized using Ti-bearing blast furnace slag as a low-cost and environmentally friendly starting material. The as-synthesized TiO_2 was the well crystallized rutile phase and consist of uniform separated hollow spheres. In addition, the sphere wall of hollow spheres is composed of nanoparticles. Almost complete extraction of Ti from TFS is achieved under optimal conditions in NaOH-NaF molten salt system, and that conditions are a temperature of $500\text{ }^\circ\text{C}$ a liquid-to-solid mass ratio 3:1, a NaOH-to-NaF molar ratio of 3:1 and a slag size of $45\text{-}75\text{ }\mu\text{m}$. The kinetic analysis indicated that the slag decomposition process was applied to the shrinkage nucleus model, and the reaction process was controlled by chemical reaction. The apparent activation energy of the reaction was 39.54 kJ mol^{-1} .

Acknowledgments

The authors acknowledge the financial support of the National Natural Science Foundation of China (No.U1360204 and No.51304139); Liaoning Province Education Administration LG201918); Natural Science Foundation of Liaoning Province(20180550902 and 2019-ZD-0258).

References

- [1] J. Yang, S. Lei, J. Yu, G. Xu, Journal of Environmental Chemical Engineering **2**(2), 1007(2014).
- [2] X. F. Lei, X. X. Xue, H. Yang, Transactions of Nonferrous Metals Society of China **22**(7), 1771(2012).
- [3] X. F. Lei, X. X. Xu, Materials Chemistry and Physics **112**(3), 928(2008).

- [4] L. L.Sui, Y. C. Zhai, Transactions of Nonferrous Metals Society of China **24**(3), 848(2014).
- [5] X. Liu, G. Gai, Y. Yang, Z.Sui, L.Li, N.Feng, The Journal of china University of Mining and Technology **18**(2), 275(2008).
- [6] J.Lei, J.Yang, J.Yu, Y.Liu, G.Xu, CIESC Journal **65**(4), 1251(2014).
- [7] Y. Xiong, C. Li, B. Liang, J. Xie, Transactions of Nonferrous Metals Society of China **18**(3), 557(2008).
- [8] Y. Xiong, C. Li, B. Liang, The Chinese Journal Process Engineering **8**(6), 1092(2008).
- [9] Z. T.Sui, P. X. Zhang, Acta Materialia **47**(4), 1337(1999).
- [10] T. P. Lou, Y. H. Li, Z. T. Sui, Acta Metallurgical Sinica **36**(2),140(2000).
- [11] M. Y. Wang, X. W. Wang, Y. H. He, T. P. Lou, Z. T. Sui, Transactions of Nonferrous Metals Society of China **18**(2), 460(2008).
- [12] L. Zhang, L. N. Zhang, M. Y. Wang, G. Q. Li, Z. T. Sui, Minerals Engineering **20**(7), 684(2007).
- [13] W.Zhang, L.Zhang, J. H.Zhang, N. X. Feng, Industrial & Engineering Chemistry Research **51**(38), 12294(2012).
- [14] W. Zhang, L. Zhang, N. X. Feng, Advanced Materials Research **641-642**, 363(2013).
- [15] X. Lu, G. Wang, T. Zhai, M. Yu, J. Gan, Y. Tong, Y. Li, Nano Letters **12**(3), 1690(2012).
- [16] B. Liu, Y. Huang, Y. Wen, L. Du, W. Zeng, Y. Shi, F. Zhang, G. Zhu, X. Xu, Y. Wang, Journal Materials Chemistry **22**(15), 7484(2012).
- [17] A. K.Rai, L. T. Anh, J. Gim, V. Mathew, J. Kang, B. Joseph, ElectrochimicaActa **90**, 112(2013).
- [18] A. Kumar, Anuj A. Madaria, C. Zhou, Journal Physical Chemistry C **114**(17), 7787(2010).
- [19] S. He, H.Sun, D.Tan, T. Peng, Environmental Sciences **31**, 977(2016).
- [20] B. Liu, H. Du, S. Wang, Y. Zhang, S. Zheng, L. Li, D. Chen, AIChE Journal **59**(2), 541(2013).
- [21] Y. Zhang, S. L.Zheng, H. B.Xu, H.Du, International Journal Mineral Processing **95**(1-4), 10(2010).